The Modelling of Semiflexible Conveyor Structures for Coal-face Steering Investigations

PART I: SPATIALLY DISCRETE MODELS

Edwards J.B.*, Wolfenden, R.A.† and Yazdi, A.M.S.R.*

April 1981

One of a pair of companion papers submitted to the Institution of Mechanical Engineers for publication in the Proceedings.

* Department of Control Engineering, University of Sheffield.

† Mining Research and Development Establishment, National Coal Board.

The modelling of semiflexible conveyor structures for coal-face steering investigations

PART I SPATIALLY-DISCRETE MODELS

Edwards, J.B.[*], Wolfenden, R.A.[†], and Yazdi, A.M.S.R.[*]

1. Introduction

1.1 The power-loader and conveyor

Fig. 1 illustrates diagramatically a short section of a modern longwall coal-face installation in plan-and side-views. The coal-cutting machine shown is of the popular ranging-drum shearer type. The machine both cuts the coal from the solid face as it proceeds along the face (from left to right in Fig. 1) and simultaneously loads the product onto the scraper-chain conveyor. This operation is aided by the spiral vanes around the rotating drum periphery upon which the cutting picks are mounted. Because of its dual function, the machine is described colloquially as a cutter-loader or sometimes a power-loader. The scraper-chain conveyor also has more than a single function: It not only conveys the cut product to the face-end but, because of the robust construction its structure, it also provides a comparatively smooth track upon which the power-loader rides, as shown in Fig. 1. The power-loader actually slides on skids along the side-channels of the conveyor, traction being provided increasingly nowadays by a rack-and-pinion drive, the rack being bolted to the conveyor structure.

Between consecutive cuts made along the face, typically 100 to 200m in length, the conveyor is snaked forward onto the newly-cut floor as indicated. Horizontal rams attached to and powered from the line of roof-support units behind the conveyor and not shown in Fig. 1 are used

* Department of Control Engineering, University of Sheffield

† Mining Research and Development Establishment, National Coal Board

to advance or push-over the conveyor, and by reversing the jack action, the roof-supports, lowered one at a time, are then themselves drawn forward using the conveyor structure as an anchor beam. The conveyor structure must therefore be extremely robust to withstand the point loads of several tons imposed on it both horizontally and vertically and yet sufficiently flexible to allow a short snaking distance and so minimise the area of newly exposed roof left unsupported. Because of these key properties, the conveyor is generally termed, in full, the armoured-flexible-conveyor , and abbreviated to a.f.c.

Flexibility is also required in the vertical plane as indicated in exaggerated fashion in the side-elevation of Fig. 1. This is because of coal-seam undulation and the need to change the cutting horizon within a seam from time to time as coal quality at different levels in the seam varies. To regulate against seam unudlations or to accomplish definite prescribed vertical manoeuvres of the entire installation within the seam, vertical steering facilities must be provided and this is one purpose of the ranging boom upon which the cutting drum is mounted. Control may be manual or automatic and in Fig. 1 a nucleonic floor-sensor of the backscatter type[1] is illustrated for measurement of the floor-coal thickness left some distance X behind the drum. More conventionally, a roof-sensor is employed since the penetration of fragile roof-strata can quickly bring about serious roof-collapse. Technically the two problems are little different and floor-control is slightly simpler to present and is therefore the case considered here. Clearly roof-or floor-sensor measurements can provide the basic feedback signal for automatic control of the hydraulically-powered steering boom.

1.2 The steering system model

Fig. 2 shows the behaviour of the power-loader and a.f.c. in end-elevation (i.e. looking in the so-called along-face direction) The machine geometry is arranged so that, with the steering boom centralised, the drum cuts at the level of the front edge of the a.f.c. but in response to a step created by a boom deflection, the a.f.c. undergoes a tilt-change in the face-advance direction since the a.f.c. width, W_c and the drum width, W_d are always subject to the inequality

$$W_c > W_d \tag{1}$$

For simplicity of presentation we shall assume

$$W_c = W_d(1 + \varepsilon) \tag{2}$$

where

$$0 < \varepsilon << 1.0 \tag{3}$$

so that in the development of the process equations we may make the approximation

$$W_c \simeq W_d = W \tag{4}$$

without eliminating the tilt-change effect.

A model for the vertical steering process can be derived from the application of small-angle geometry to Figs. 1 and 2. If, as indicated n denotes the cut- (or pass-) number, and ℓ the distance of the drum from the left-hand face-end, then the following relationship between the various heights and tilts of machine and a.f.c are readily deduced:

$$y(n,\ell) + z(n,\ell) = h(n,\ell+R) + W\alpha(n,\ell+R) + R\beta(n,\ell+R) + J(n,\ell) \tag{5}$$

where face-advance tilt α, in radians, is given by

$$\alpha(n,\ell) = \{h(n,\ell) - h(n-1,\ell)\}/W \tag{6}$$

and along-face tilt β, also in radians, by

$$\beta(n,\ell) = \{h(n,\ell) - h(n,\ell+F)\}/F \tag{7}$$

assuming skids A,B and C are trapped in permanent contact with the a.f.c.

In these equations h denotes the height of the a.f.c., z the height of the lower coal/stone interface (parting) and y the thickness of the coal-floor left by the cutting-drum. J is the deflection of the cutting-drum, R the length of the boom and F the skid spacing along-face.

A conventional analogue control law takes the form

$$J_d(n,\ell) = k_h\{y_r - y_m(n,\ell)\} - k_g W\alpha(n,\ell+R) \quad (8)$$

where J_d is the demanded drum deflection applied to the hydraulic servo driving the steering boom which can be usually modelled sufficiently accurately by a simple first-order lag relationship:

$$dJ(n,\ell)/d\ell = (1/X_2)\{J_d(n,\ell) - J(n,\ell)\} \quad (9)$$

i.e. $$J(n,\ell) = J_d(n,\ell)/(1+X_2D) \quad (10)$$

where $$D \equiv d/d\ell \quad (11)$$

and X_2, assuming a constant machine speed v, is simply the servo time-constant multiplied by v.

In control law (8), y_r is the constant desired floor-coal-thickness, $y_m(n,\ell)$ the measurement obtained from the floor-sensor and k_h and k_g are the preset height-and tilt-gains of the controller. Because of the measurement delay X and the sensor time-constant† X_1/v, y_m is related to y thus

$$d\,y_m(n,\ell)/d\ell = (1/X_1)\{y(n,\ell-X) - y_m(n,\ell)\} \quad (12)$$

or, in operational form

$$y_m(n,\ell) = y(n,\ell-X)/(1+X_1D) \quad (13)$$

1.3 The overall process model structure

The process model is, of course, incomplete without a relationship describing how the a.f.c. moulds itself to the cut floor i.e. a relationship between front and rear conveyor edge heights $h(n+1,\ell)$ and $h(n,\ell)$ and the cut-floor heights $y(n,\ell)$ and $y(n-1,\ell)$ upon which the

† A substantial time-constant is generally necessary to smooth out the strong random component of the sensor signal arising from the use of radio isotopes of very low strength in these transducers. This is essential for reasons of safety and health.

a.f.c. rests after pushover. Such a model will be a two-input two-output process, since the stiffness of the a.f.c. deck-plate will cause some interaction between $h(n+1,\ell)$ and $y(n-1,\ell)$ and between $h(n,\ell)$ and $y(n+1,\ell)$. Fig. 3 represents the overall system in block-diagram form and split into two distinct but interconnected subsystems:

(i) the machine-steering process

and (ii) the a.f.c. floor-fitting process

The machine-steering process is fully described by equations (5) to (8), (10) and (13) and its internal structure, derived directly from these equations, is shown in Fig. 4. The development of a model for the a.f.c. floor-fitting process is the first objective of this and a companion paper. The second objective is to explore the stability and performance of the composite system.

Investigations of the dynamic behaviour of the system have hitherto been of three types, these being

(a) simulation studies

(b) analytical calculation

and (c) field trials

Field trials are enormously expensive undertakings in industry generally and in coal mining this problem is particularly accute because of the very high level of electronic and mechanical engineering which must be invested in the development of robust instruments, controllers and data-links for the acquisition of even the simplest data. Such equipment must not only withstand the arduous coal-face environment, but must be safe in all respects. Equipment must be flameproof or intrinisically-safe to avoid any risk of methane ignition and must be highly fault-tolerant if included in any control loop. Production losses through failure of prototype equipment can rarely be tolerated and even the measurement of distance, ℓ, travelled is far from being a trivial exercise.

Simulation and analysis are therefore particularly crucial in coal-face control studies.

Because of the absence of a sound mathematical model for the a.f.c fitting process, simulation has hitherto been a tedious exercise requiring the use of instrumented mechanical models for simulation of a.f.c. behaviour (2), with all the attendant problems of geometric scaling. The exploration of a wide range of control and process parameters and structures has therefore been prohibitive and to alleviate this problem the authors have addressed themselves to the development of a soundly-based computer simulation of the conveyor.

In analysis, simple intuitive models of the a.f.c. fitting process have been adopted, frequently producing alarming results. The simplest model has been based on the so called 'rubber conveyor' assumption which permits the a.f.c. to mould itself precisely to the previously-cut floor i.e.

$$h(n+1,\ell) \simeq y(n,\ell) + z(n,\ell) \qquad (14)$$

Using this and linear analytic a.f.c. models of somewhat greater complexity, e.g.

$$h(n+1,\ell) = G_c(D)\{y(n,\ell) + z(n,\ell)\} \qquad (15)$$

where $G_c(D)$ is some rational transfer-operator, stability studies can be quickly undertaken often by pencil-and-paper methods (4),(5) as illustrated by the example in the following Section.

1.4 Example of behaviour prediction by analysis

Suppose for simplicity we neglect hydraulic lag X_2 and set $k_g = 1.0$ so eliminating the effect of tilt $\alpha(n,\ell+R)$ on $y(n,\ell)$, (see Fig. 4). Suppose also we restrict our attention to so-called fixed-drum machines where offset R = 0 and steering is achieved by pitching or rolling the entire machine body about an underframe trapped to the a.f.c. The effect of tilt $\beta(n,\ell+R)$ is thus removed likewise and the overall system block-diagram reduces to the form shown in Fig. 5 and the machine steering model becomes that shown in Fig. 6. For stability studies external inputs y_r and $z(n,\ell)$ may be disregarded so that for the steering system we have

$$y(n,\ell) = G_s(D)\ h(n,\ell) \tag{16}$$

where $G_s(D)$, in this simple case is given by

$$G_s(D) = \frac{1+X_1 D}{1+X_1 D+k_h \mathrm{Del}(X)} \tag{17}$$

where Del(X) denotes a distance shift X, whilst, for the a.f.c., we have

$$h(n+1,\ell) = G_c(D)\ y(n,\ell) \tag{18}$$

Now merely making $G_s(D)$ a stable process (by suitable choice of k_h and possibly X_1) will only ensure single-pass stability and for the stability of the multipass process we must ensure that signals of any frequency ω be attentuated in passing round the loop of Fig. 5. Hence, for multipass stability

$$|G_s(j\omega)|\,|G_c(j\omega)| < 1.0 \quad , \quad \text{all } \omega \tag{19}$$

Now if we assume the rubber conveyor model to apply, then from (14), with z neglected, we deduce

$$G_c(j\omega) = 1.0 \tag{20}$$

so that for stability

$$|G_s(j\omega)| < 1.0 \quad , \quad \text{all } \omega \tag{21}$$

and from (17), in our example

$$G_s(j\omega) = \frac{1+X_1 j\omega}{1+X_1 j\omega + k_h \exp(-Xj\omega)} \tag{22}$$

so that

$$|G_s(j\omega)| = \sqrt{\frac{1+(X_1\omega)^2}{1+(X_1\omega)^2 + k_h^2 + 2k_h(\cos X\omega - X_1\omega \sin X\omega)}} \tag{23}$$

The spectrum of $|G_s(j\omega)|$ computed from (23) is shown for $k_h = 0.5$ in Fig. 7 for a range of values of X_1/X from which it is deduced that only for very small values of steering gain k_h and prohibitively large ratios X_1/X can condition (21) be satisfied so that if the true a.f.c. does indeed resemble the conceptual rubber conveyor in its behaviour, then instability is inevitable with this form of control. Simulation confirms this prediction as illustrated in Fig. 8 (for which $k_h = 0.8$, $k_g = 1.0$, $X = 1.25$m, $X_1 = 0.6$m, $X_2 = 0.165$, $R = 0$).

It is fairly readily shown that making $R > 0$, varying k_g and making X_2 non-zero offer no cure for the repeated excitation of the $G_s(D)$ resonance, in fact such changes have an adverse effect on multi-pass stability. Indeed only by recourse to control from a previous pass measurement so that

$$y_m(n,\ell) = y(n-1,\ell)/(1+X_1D) \qquad (24)$$

can stability be achieved with the rubber conveyor model. Since the coal-sensor cannot be sited in the previous pass due to obstruction by a.f.c or roof-bars, expensive stored-data computer-control is the only way of implementing equation (24). Pending the development, proving and exploitation of such a scheme there is therefore great incentive to explore the nature and effect of $G_c(D)$ or, more precisely, the response of the a.f.c to the undulating floor beneath it. The present paper is concerned with the development of a rigorous computer simulation model for the a.f.c and a companion paper with an acceptable linear transfer-operator, $G_c(D)$ for analytical studies.

2. Conveyor modelling

2.1 Early empirical methods

To avoid the need for scale-models in system simulation, early attempts at estimating the fit of the a.f.c to the cut-floor {produced by computer simulation of $G_s(D)$} involved the skills of a draughtsman.

He would be supplied with the recorded cut-floor profiles beneath front and rear edges to which he would attempt to determine a realistic fit, by eye. The two piecewise-linear a.f.c. edge profiles thus produced would then be fed as input data to the next run of the simulation of $G_s(D)$. Attempts[6] were made in later investigations to programme the draughtsman's rules of thumb in an attempt to eliminate this, time-consuming manual stage of simulation. Some success was achieved but highly undulating floors produce high interaction across a considerable number of neighbouring a.f.c. trays so requiring a great deal of iteration and ultimately producing much uncertainty as to the reliability of the elementary fitting logic. Other attempts involved the conceptual sub-division of trays into say, ten or more, semi-independent sub-sections, the behaviour of which was limited by much empiricism. Far from producing good practical responses however, such programs generated highly impractical spiky waveforms which became accentuated with each successive pass. It was eventually realised that a.f.c. modelling should be attempted on a much sounder basis, undertaken at Sheffield University and sponsored by the N.C.B., and a description of this attempt now follows.

2.2 The use of general dynamic programming

The a.f.c. will settle on the cut floor to a condition of minimim energy. The free angular play between the I consecutive trays may therefore by regarded as the I control vectors of an energy-minimising optimal control problem subject to various height-(state-) and angular (control-) constraints. Now whereas these constraints render true analytic solution very difficult, they greatly assist numerical solution since they drastically reduce the area of state-space (i.e. range of tray-heights) over which an optimum need be sought. The technique ideally suited to this type of problem is therefore that of general dynamic programming. The realisation of these elementary facts; so obvious with hindsight, has made possible a complete breakthrough in the problem of a.f.c. modelling.

To illustrate the method, each a.f.c. tray is, for the moment regarded as having completely rigid side-channels and a completely flexible (rubber) deck-plate so that the problem reduces to fitting two independent-(uncoupled-) chains of stiff rods, each to a single-line floor-profile beneath. The free angular movement between 'rods' is regarded as being hard-limited, in the along-face direction , within the range $\pm\Delta\gamma$.

Fig. 9 illustrates the variables involved in the fitting problem and the following equations interrelate these variables. The tray joint-heights are, working backwards from the R.H. face-end, $h(0)$, $h(1)$, $h(2)\ldots h(i)\ldots h(I)$ and in terms of our earlier notation, but dropping pass number n,

$$h(i) \equiv h(L-i\,X_p) \qquad i = 0,1,2\ldots I \tag{25}$$

where L = the face-length and X_p = a tray-length so that

$$I = L/X_p \tag{26}$$

Relating consecutive joint-heights and rod-tilts $\gamma(i)$ we have that

$$h(i-1) = h(i) + X_p\,\gamma(i) \tag{27}$$

if the angles are small, and the rod height $h(\ell)$ at any point distant ℓ from the L.H. end may be expressed in terms of joint-height and rod-tilt thus

$$h(\ell) = h(i) + (\ell-L+i\,X_p)\gamma(i), \quad L-i\,X_p < \ell < L-(i-1)X_p \tag{28}$$

Now the rods must not penetrate the cut floor profile $y(\ell)$ so that

$$h(\ell) \geq y(\ell) \quad , \quad o < \ell < L \tag{29}$$

and furthermore the angular freedom $\pm\Delta\gamma$ between consecutive rods must not be exceeded so that

$$|\gamma(i) - \gamma(i-1)| \leq \Delta\gamma \quad , \quad i = 2,3\ldots I \tag{30}$$

Assuming no yield of either the rods or the cut-floor the chain of rods will settle to a profile defined by a height sequence h(o), h(1), h(2)....h(I) such that the total potential energy of the chain is a minimum subject to the two constraints (29) and (30). Now if the energy of the ith rod is δE_i, this is given by

$$\delta E_i = mg\{h(i) + h(i-1)\}/2, \quad i=1,2,...I \tag{31}$$

where 2 m is the mass of one tray of the a.f.c., and the total potential energy of the last i rods is therefore

$$E_i = \sum_{j=1}^{i} \delta E_j \tag{32}$$

Now for a given h(i), E_i is a function of h(i) and the tilts $\gamma(1)...\gamma(i)$ and the minimum value $E_i^*\{h(i)\}$ may therefore be obtained in principle, by minimising E_i with respect to the sequence of variables $\gamma(1)...\gamma(i)$ i.e.

$$E_i^*\{h(i)\} = \min_{\gamma(1),\gamma(2)...\gamma(i)} \left[E_i\{h(i),\gamma(1),\gamma(2)...\gamma(i)\}\right] \tag{33}$$

Minimising E_i in the manner implied by (33) would be enormously time consuming however because of the vast field of search involved. Instead, this multistage design process (an I-stage process for all I rods) may be reduced to I much simpler single-stage decision processes by utilising the equation of General Dynamic Programming, viz:

$$E_i^*\{h(i)\} = \min_{\gamma(i)} \left[\delta E_i\{h(i),\gamma(i)\} + E_{i-1}^*\{h(i-1)\}\right] \tag{34}$$

Thus, starting with the rightmost rod (i=1), $E_1^*\{h(1)\}$

is readily computed for a range of initial heights h(1) by finding, for each h(1) chosen, that value of $\gamma(1)$ which minimises δE_1 {calculated from (27) and (31) with i set to 1.0} subject to the constraint (29).

$E_o^*\{h(o)\}$ may of course be set to zero in (34) for this one-step optimisation. A table of E_1^* versus h(1) may thus be computed and stored, along with associated values of the optimising tilt $\gamma^*(1)$ for each h(1) chosen.

A table of E_2^* versus h(2) may now be computed using (34) since values of E_1^* are now known directly or by interpolation for each h(2) and $\gamma(2)$ selected. For each h(2), the full range of $\gamma(2)$ allowed by the constraints (29) and (30) is explored and the value $\gamma^*(2)$ giving <u>minimum</u> $\delta E_2 + E_1^*$ $(=E_2^*)$ thus found.

From the E_2^* versus h(2) table and similar computations based on equation (34), E_3^* may be found and the whole process repeated incrementing i through from 1 to I whereupon tables of $E_i^*\{h(i)\}$ and $\gamma_i^*\{h(i)\}$ for $1 < i < I$ are obtained. For any selected initial condition h(I) therefore, by repeated use of the γ_i^* tables and equation (27) the optimal height- and tilt-profiles h(I), h(I-1)...h(o) and $\gamma^*(I)$, $\gamma^*(I-1)$... $\gamma^*(1)$ may be immediately obtained. The fit will be accurate to within the resolution of the height and tilt increments chosen and provided attention is restricted to increments of say 1% of the maximum floor wave amplitude and 1% of $\Delta\gamma$ (i.e. 100 increments of height x 200 increments of angle) at each joint, problems of computer storage and execution time are unimportant. Using a FORTRAN IV program on an Interdata 3220 computer, a 10-tray, (100-sample) 20-pass simulation using a height range of ±15cm in steps of 0.5cm and 60 angular increments, some 8 k-words of storage were found to be necessary (5k-words for data). The program was written in floating point arithmetic, requiring ten minutes for the 20-pass simulation. Recourse to fixed-point arithmetic would obviously have produced a far faster program execution.

Fig. 10 flow-charts the sequence of computations outlined qualitatively above for the general, ith rod.

3. Results

The two-dimensional* fitting routing described above was tested by subjecting the entire steering system simulation to an initially disturbed cut floor profile. The coal seam was assumed to be flat, i.e. $z(n,\ell) = o$ for all n and $o < \ell < L$ and the attempts of the automatic steering to restore the a.f.c to a flat horizon at $y(n,\ell) = 0$ were observed. Fig. 11 shows the results obtained over a sequence of 14 passes for the following system parameters:

$X/X_p = 0.70$	$R = 0.0$
$X_1/X_p = 0.50$	$W_c = W_d = W$
$X_2/X_p = 0.25$	$\Delta\gamma . X_p = 10cm$
$k_h = 0.50$	resolution = 0.25 cm
$k_g = 1.00$	$\Delta X/X_p = 0.1$ (ΔX = step length)

Traces for the cuts 0 to 4 illustrate the quality of the a.f.c. fit produced by the dynamic programming. Accepting the 0.25cm resolution, the routine is clearly successful and its predictions, as regards quality of fit, difficult to challenge on empirical grounds. (The gross inflation of the vertical height scale with respect to the horizontal scale in Fig. 11 should, of course, be noted: this is the explanation for the apparent variation in tray-lengths in Fig. 11. In practice the small-angle assumption would not be contravened and, by plotting to equal scales, this apparent phenomenon would not appear).

Somewhat harder to accept is the overall system behaviour over a large number of passes. By cuts five and six, a flatter cutting horizon has been produced but with subsequent passes significant deterioration takes place. Regarding lag X_1 as a small additional delay, so that the net system delay becomes $X + X_1$ (and hence the natural frequency of the

* The fitting problem has here been reduced to a <u>two dimensional problem</u> in that interaction between the two a.f.c. side channels via the deck-plate has been neglected.

steering system is $1/2(X+X_1)$) so that its natural cycle-distance is $2(X+X_1) = 2.4$ tray-lengths in this example. Oscillations of this frequency are clearly developing by cut 14 (and indeed continue to grow in amplitude at this frequency thereafter) so that we must conclude that piecewise rigidity of the a.f.c. sides is, unfortunately, not a significant stabilising influence though it does reduce the rate of growth of oscillations to some extent.

4. Stiffening the deck-plate

We now consider the effect of a stiff rather than a flexible deckplate so that front and back a.f.c. heights $h_f(i)$ and $h_b(i)$ are no-longer independent. In addition the associated hard constraint

$$|\alpha(i) - \alpha(i-1)| \leq \Delta\alpha, \; i = 2,3,\ldots I \quad (35)$$

on the incremental twist of the a.f.c at its joints must also be considered. Fig. 12 defines the height- and tilt-variables describing the position and attitude of the ith tray of the a.f.c. The corner heights are clearly given by

$$h_f(i) = h(i) + \alpha(i)(W/2) \quad (36)$$

$$h_b(i) = h(i) - \alpha(i)(W/2) \quad (37)$$

$$h_f(i-1) = h(i) + X_p\,\gamma(i) + \alpha(i)(W/2) \quad (38)$$

$$h_b(i-1) = h(i) + X_p\,\gamma(i) - \alpha(i)(W/2) \quad (39)$$

In the dynamic programming, the pan-centre height h(i) is now regarded as the state-variable but, unlike the two dimensional problem, there are now two controls, $\gamma(i)$ (as before) and $\alpha(i)$ (in addition). Assuming that the tray bridges all undulations between the face-and goaf*-side of the cut-floor, height constraint (29) is now replaced by

$$h_f(\ell) \geq y_f(\ell) \quad (40)$$

and

$$h_b(\ell) \geq y_b(\ell) \quad (41)$$

* The so called goaf is the area behind the a.f.c and roof supports from which coal has already been removed and in which the roof is allowed to cave in as the face advances.

where $y_f(\ell)$ and $y_b(\ell)$ are the cut-floor profiles beneath the front and rear edges.

The potential energy of pan i now becomes

$$\delta E_i = mg\{2h(i) + X_p \gamma(i)\} \tag{42}$$

so that, at first sight only the control sequence $\gamma(1)$, $\gamma(2) \ldots \gamma(i)$ would appear to affect the total energy E_i. However, in minimising E_i, constraints (35), (40) or (41) may be impinged so as to limit the range of $\gamma(i)$ which may be explored. In fact, associated with each E_i^* there will exist a floating range of optimal tilts given by

$$\alpha_1^*(i) < \alpha(i)^* < \alpha_2^*(i)$$

which must be determined for every h(i) selected by twisting the tray up and down at each $\gamma(i)$, until one or other of the constraints (35), (40) or (41) is contravened. These variable upper-and lower-limits may be denoted by $\alpha_1(i)$ and $\alpha_2(i)$ and their particular values associated with $\gamma(i)^*$ by $\alpha_1(i)^*$ and $\alpha_2(i)^*$. For checking constraint (35) it is clear that tables of $\alpha_1(i-1)^*$ and $\alpha_2(i-1)^*$ must have been carried forward from the optimisation of the i-1 step process (along with tables of E_{i-1}^* and $\gamma^*(i-1)$ and, similarly, tables of $\alpha_1(i)^*$ and $\alpha_2(i)^*$ must be carried forward for optimising the i+1 step process. The additional search procedures now involved for the i-step process are indicated in the flowchart of Fig. 13.

Fig. 14 shows the results obtained for a single pass trial of this three-dimensional fitting routine. The trace shows the a.f.c. centre-height profile $h(\ell)$ now passing through (or strictly between) the undulating floor peaks upon which $h_f(\ell)$ and $h_b(\ell)$ rest. The result given is for $W\Delta\alpha = 0.25$ cm $X_p\Delta\gamma = 10$cm. As would be expected, simulations show that as the constraint $\Delta\alpha$ is enlarged, the a.f.c centre profile settles to a generally lower position.

5. Discussion and Conclusions

We have shown that General Dynamic Programming provides a sound basis for simulating the behaviour of face-conveyors modelled as piece-wise rigid sections with limited free play at the joints. Ignoring deck-plate rigidity allows some simplification of the model and a consequent reduction in the size of the program and data-storage area required and, more importantly, in the execution time of the program. Results presented for this simplified system used in conjunction with an automatic steering system simulation predict that the piecewise rigidity of the a.f.c does not provide an adequate stabilising force over a large number of passes of the cutting machine. A program for inclusion of deck-plate stiffness has been developed and shown to produce good floor fitting. Because of the increased program execution time necessitated by the additional search operations however, multipass trials of the enhanced model are likely to be time consuming.

In view of the results obtained from the two-dimensional model however our faith in piecewise rigidity (of side-channels and/or deck-plate) as a stabilising influence on steering systems has been considerably weakened. Elastic yeild and floor degradation are factors which have so far been neglected and which are considered in a companion paper in the hope that these factors might provide the requisite damping effects.

6. References

(1) Cooper, L.R.: 'Gamma-ray backscatter gauges for measuring coal thickness on mechanised coal faces' Proc. of I.E.E. Conference on Industrial Measurement and Control by Radiation Techniques, Guildford, 1972, I.E.E. Conf. Pub. No. 84, pp. 89-93.

(2) Bogdadi, W.A. and Edwards, J.B.: 'The automatic vertical steering of a longwall coal-cutting machine - an experimental investigation', Proc. I.Mech.E., 1975, 189(32/75), pp. 187-195.

(3) Webb, R.E. and Hartley, D.: 'Evaluation of R.O.L.F. 1 shearer-loader automatic vertical steering system', N.C.B., M.R.E. Report No. 2292, Ref. No. 2, Dec. 1965.

(4) Edwards, J.B.: 'Stability problems in the control of multipass processes', Proc. I.E.E., Vol. 121, No. 11, 1974, pp. 1425-1432.

(5) Edwards, J.B., and Greenberg, J.M.: 'Longitudinal interaction in multipass processes', Proc. I.E.E., Vol. 124, No. 4., 1977, pp. 385-392.

(6) Bogdadi, W.A.,: 'Automatic control of a longwall coal cutter', Ph. D. Thesis, Dept. of Control Engineering, University of Sheffield, 1974.

7. Acknowledgements

The modelling of the a.f.c by dynamic programming was undertaken at the University of Sheffield, in the Department of Control Engineering, and financed by a grant from the Mining Research and Development Establishment of the National Coal Board. The N.C.B's permission to publish this material is gratefully acknowedged. The views expressed are those of the authors and not necessarily those of the N.C.B.

The authors are grateful also to Professor H. Nicholson for making available the computing facilities of the Dept. of Control Engineering that were used in this project.

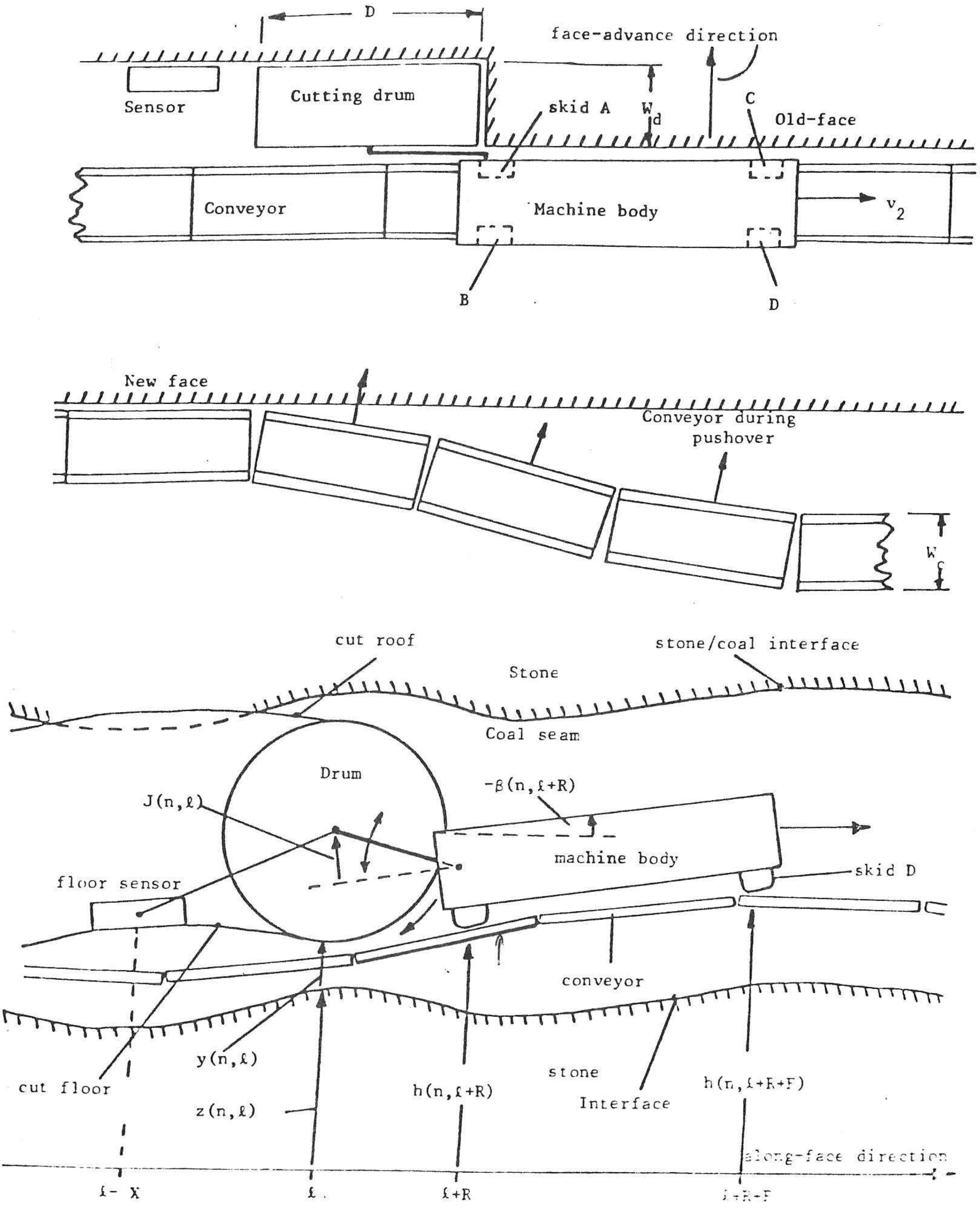

Fig. 1 Diagramatic plan and side-elevation of longwall shearer machine

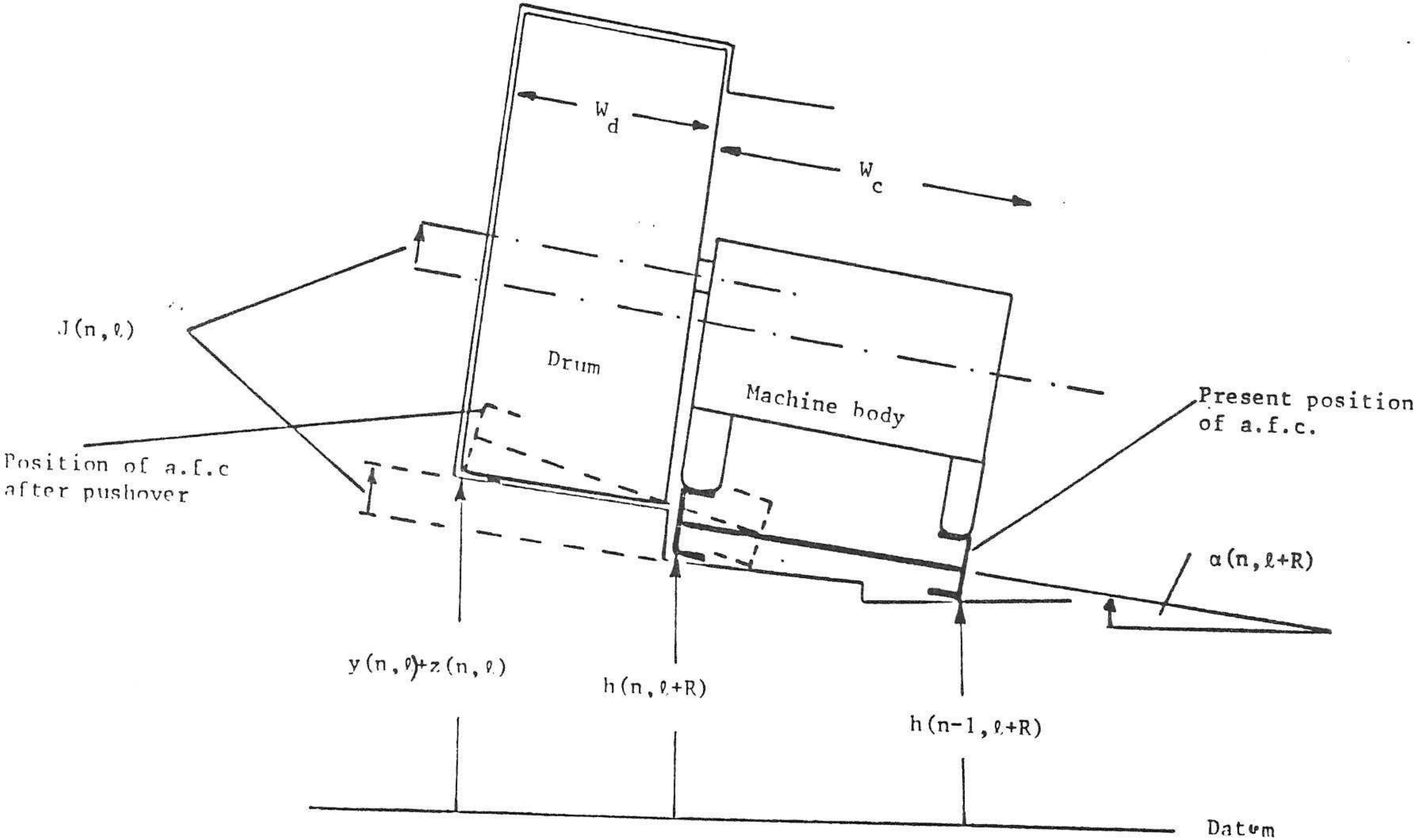

Fig. 2 Diagramatic end view of longwall shearer system.

Fig. 3 Block-diagram of interconnected a.f.c and steering models

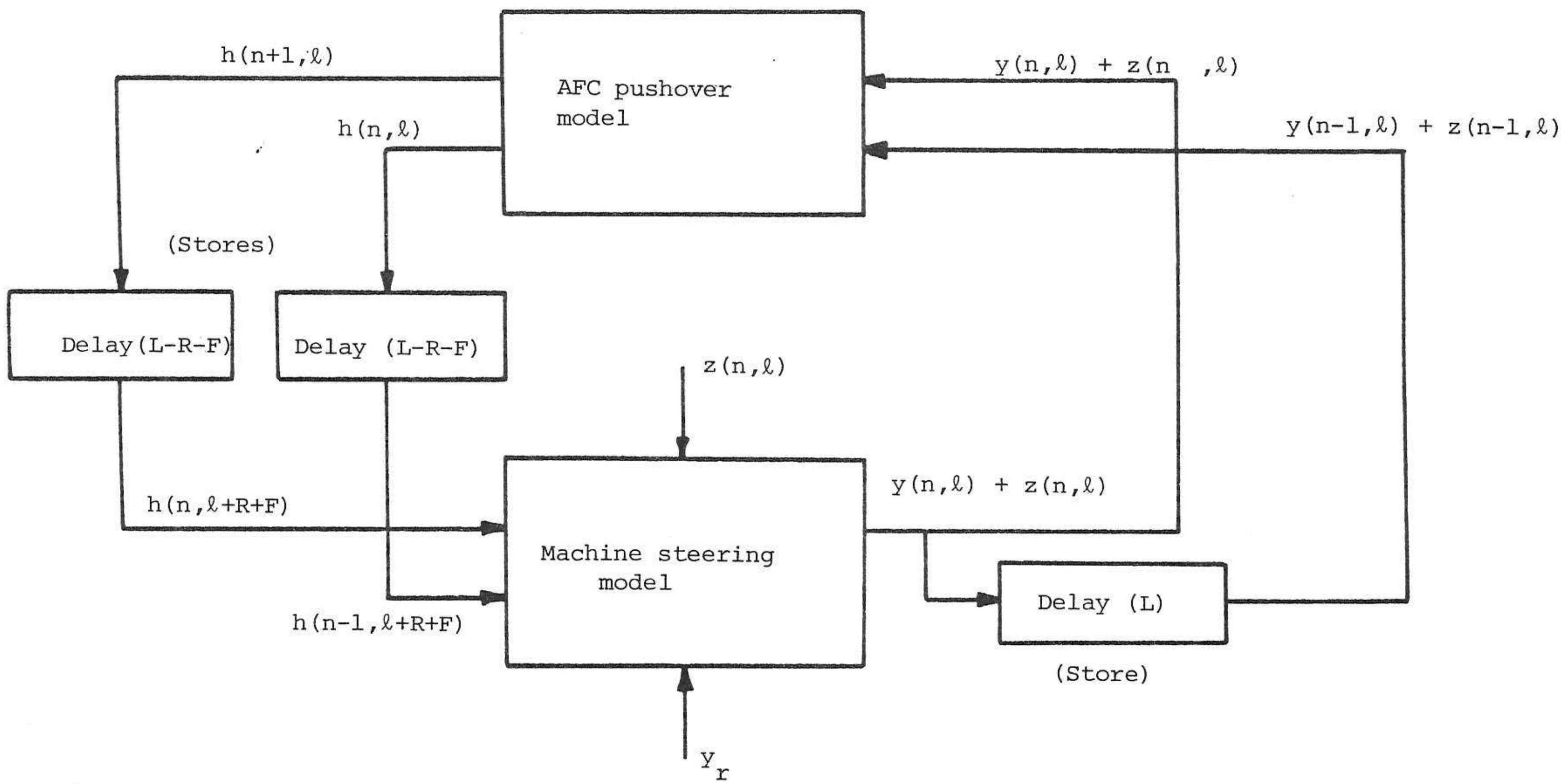

Fig. 4 Block diagram of steering system dynamics

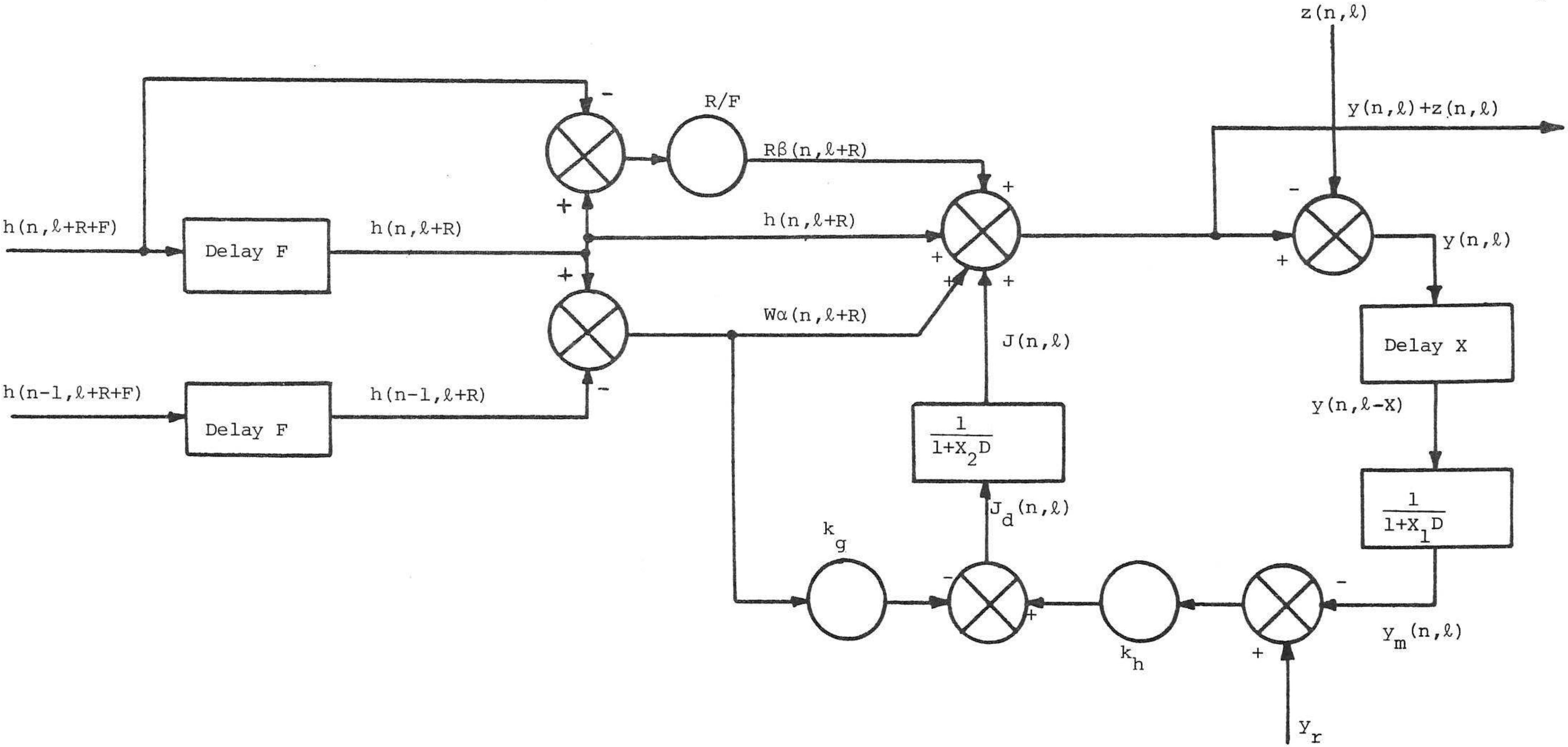

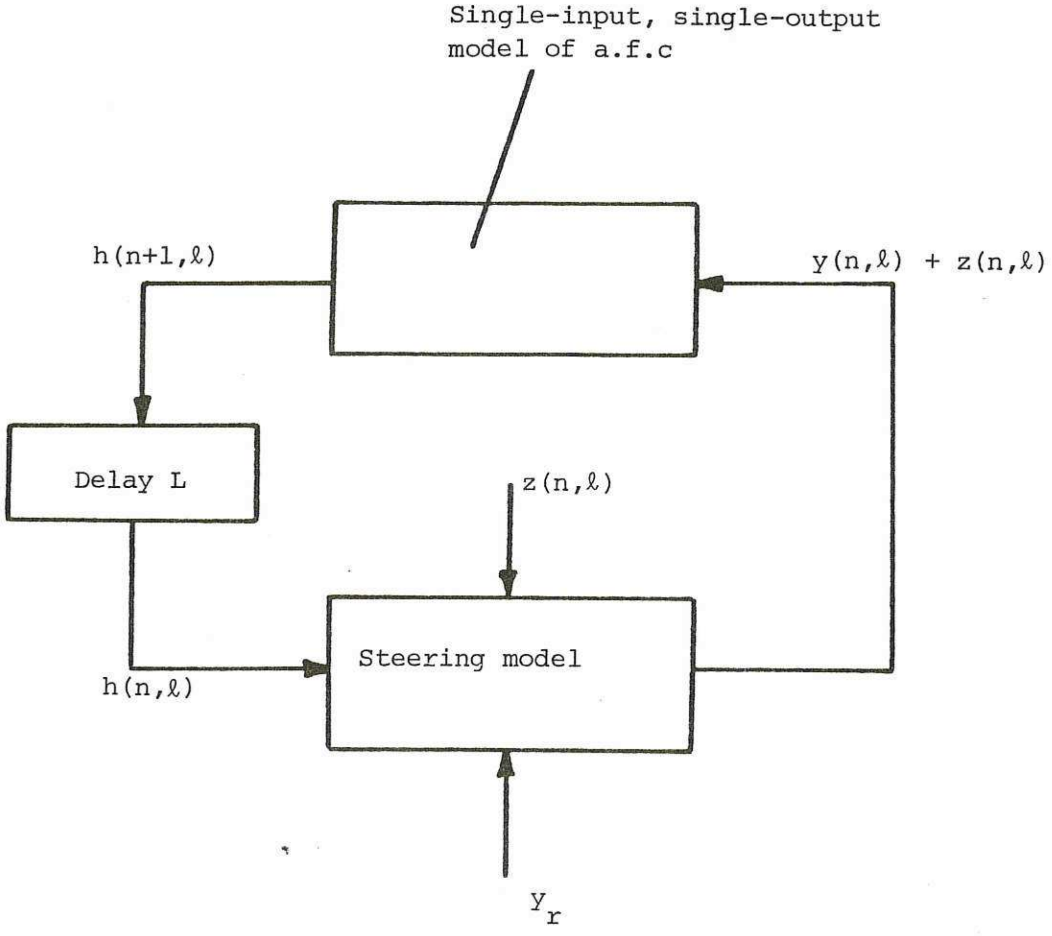

Fig. 5 Block-diagram for special case multipass system $R = X_2 = 0,\ k_g = 1.0$

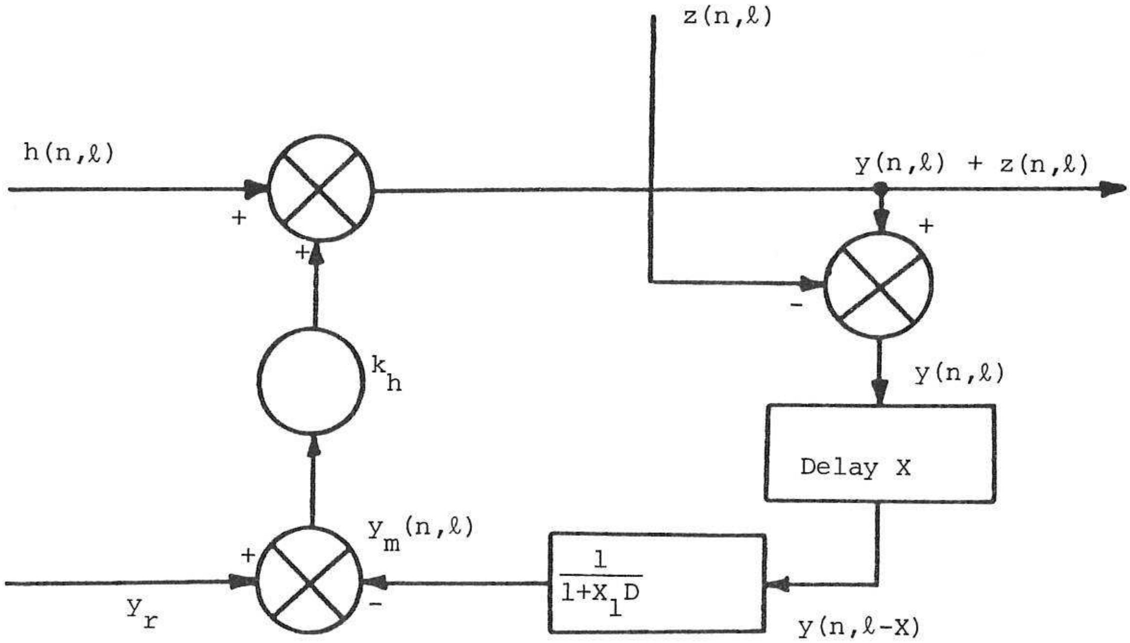

Fig. 6 Machine - steering model for special-case $R = X_2 = 0,\ k_g = 1.0$

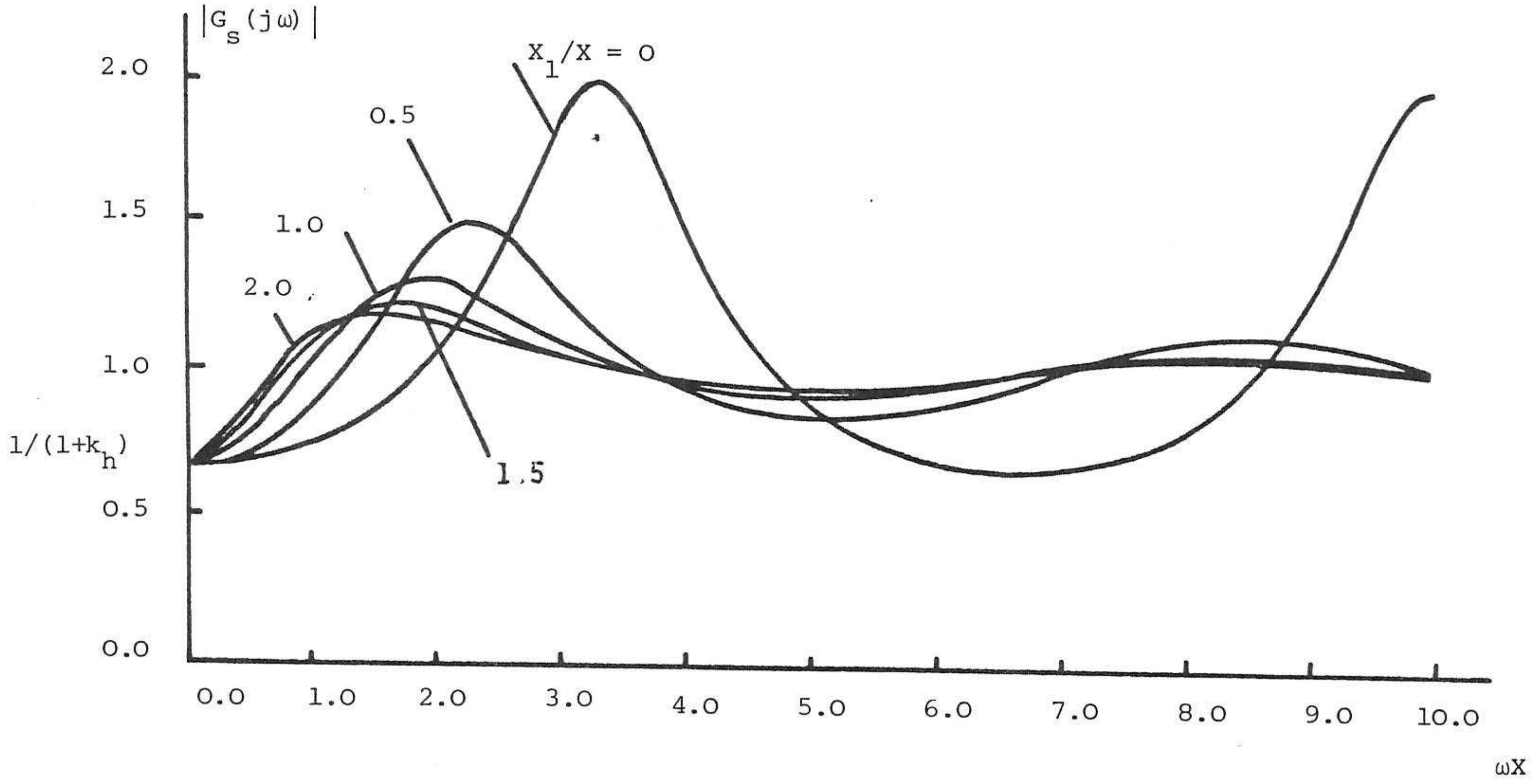

Fig. 7 Spectra of $|G_s(j\omega)|$ (k_h = 0.5,)

Fig. .8 Simulated response of rubber-conveyor model to unit downward step in coal-seam

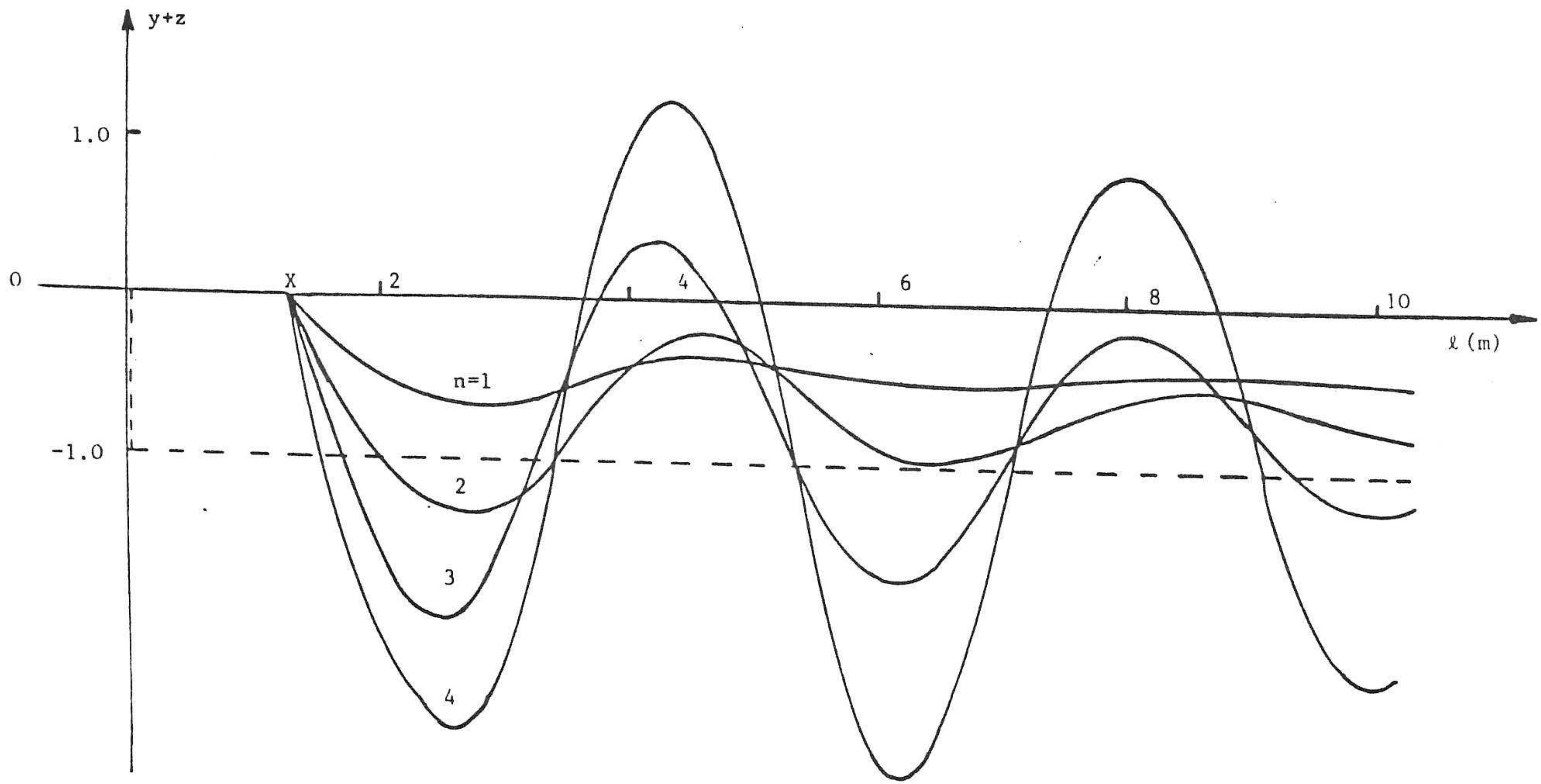

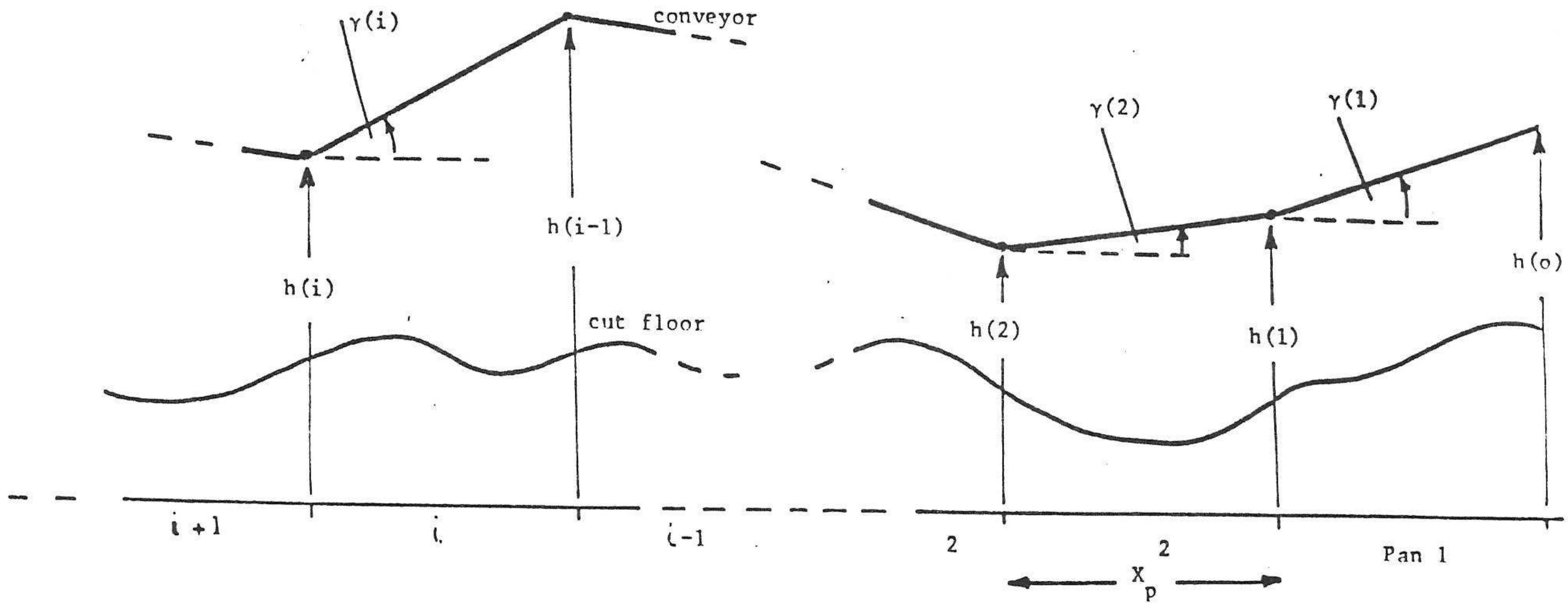

Fig. 9 Definition of variables for conveyor fitting problem.

Fig. 10 Flowchart for fitting i'th pan by dynamic programming

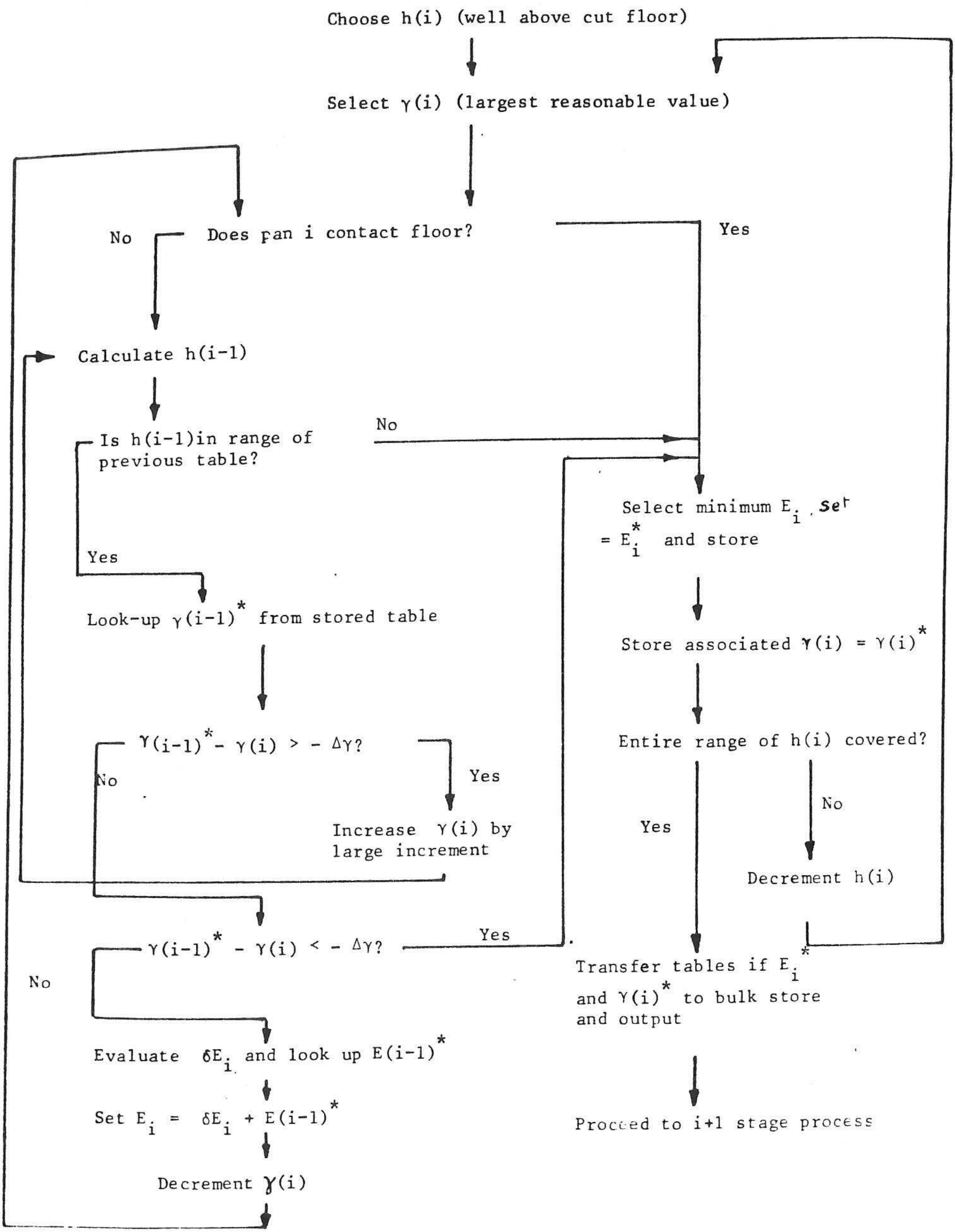

Sheet 1

Fig. 11 Multipass simulation results produced by two dimensional model

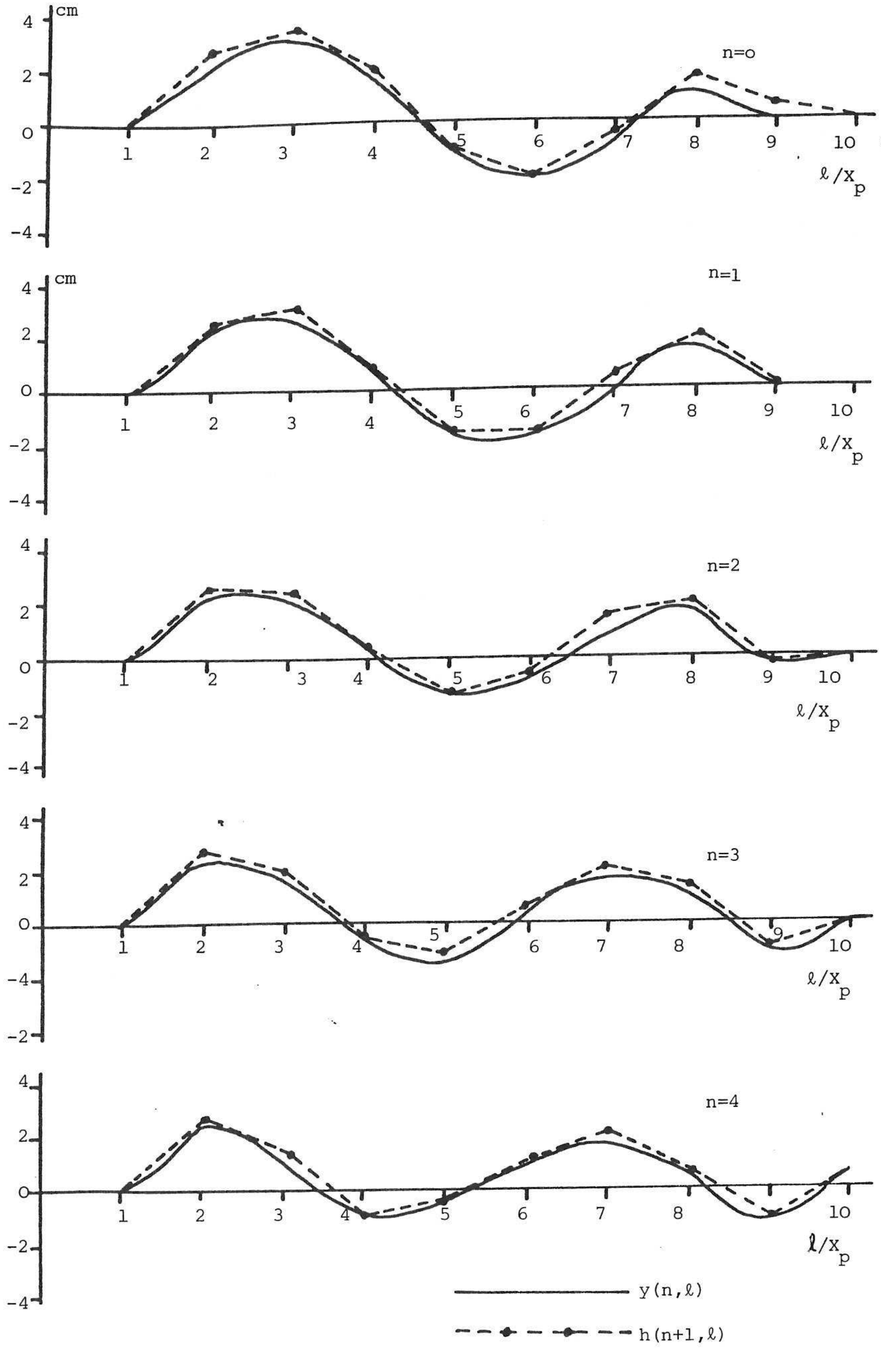

Fig. 11 (contd.)

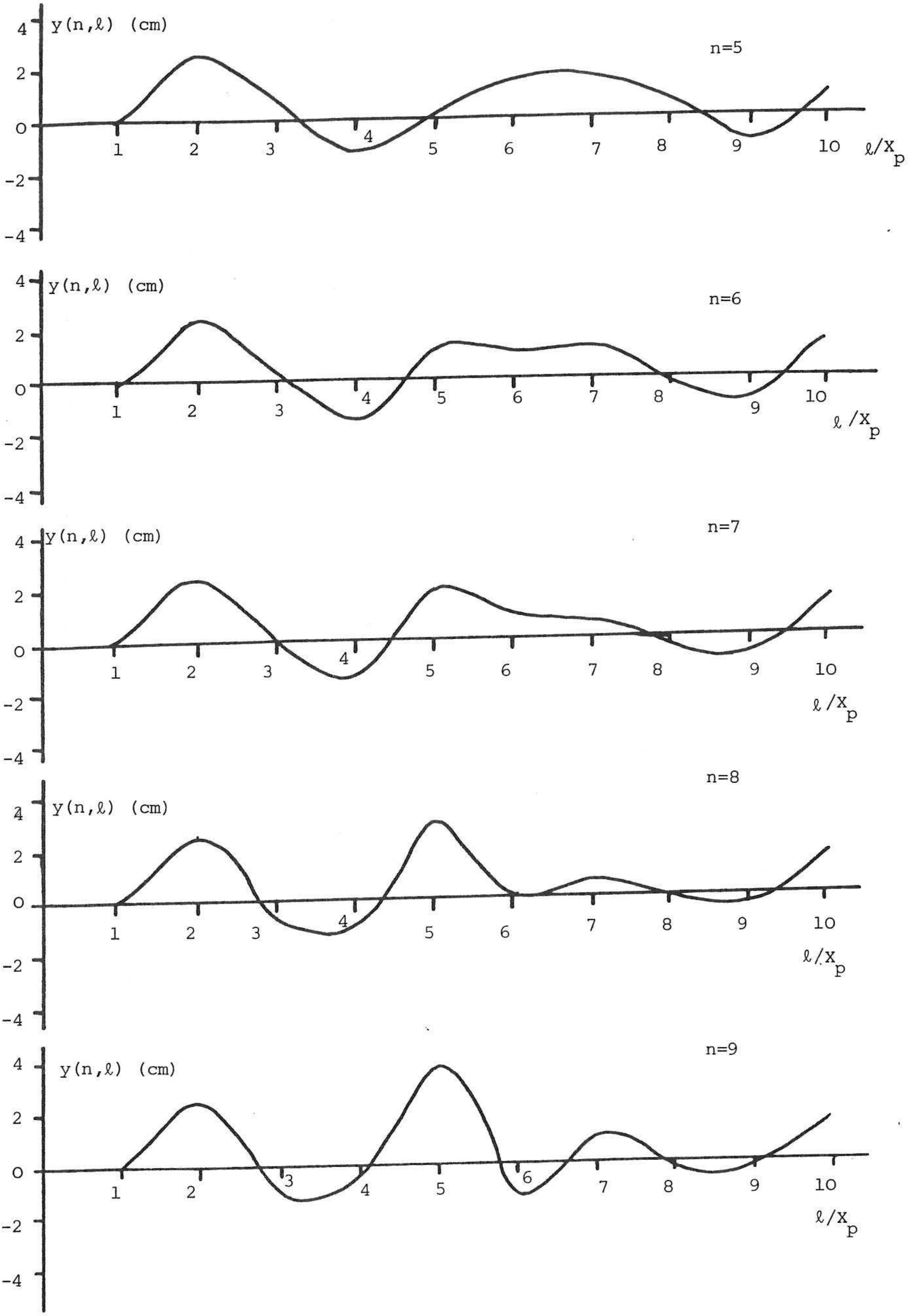
y(n,ℓ) (cm)
n=5
4
2
0
-2
-4
1 2 3 4 5 6 7 8 9 10
ℓ/X_p
y(n,ℓ) (cm)
n=6
ℓ/X_p
y(n,ℓ) (cm)
n=7
ℓ/X_p
y(n,ℓ) (cm)
n=8
ℓ/X_p
y(n,ℓ) (cm)
n=9
ℓ/X_p

Sheet 3 Fig. 11 (cont'd)

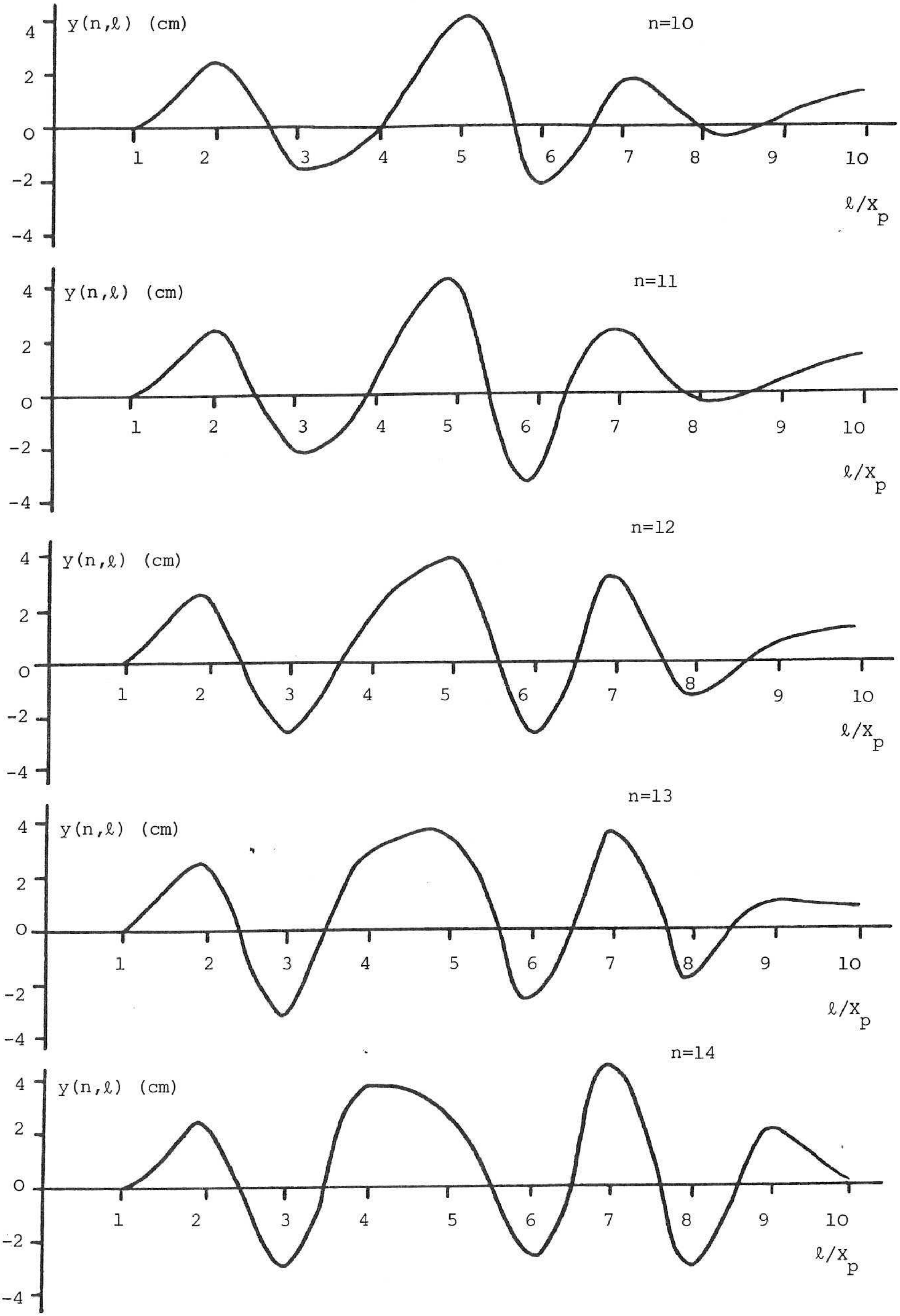

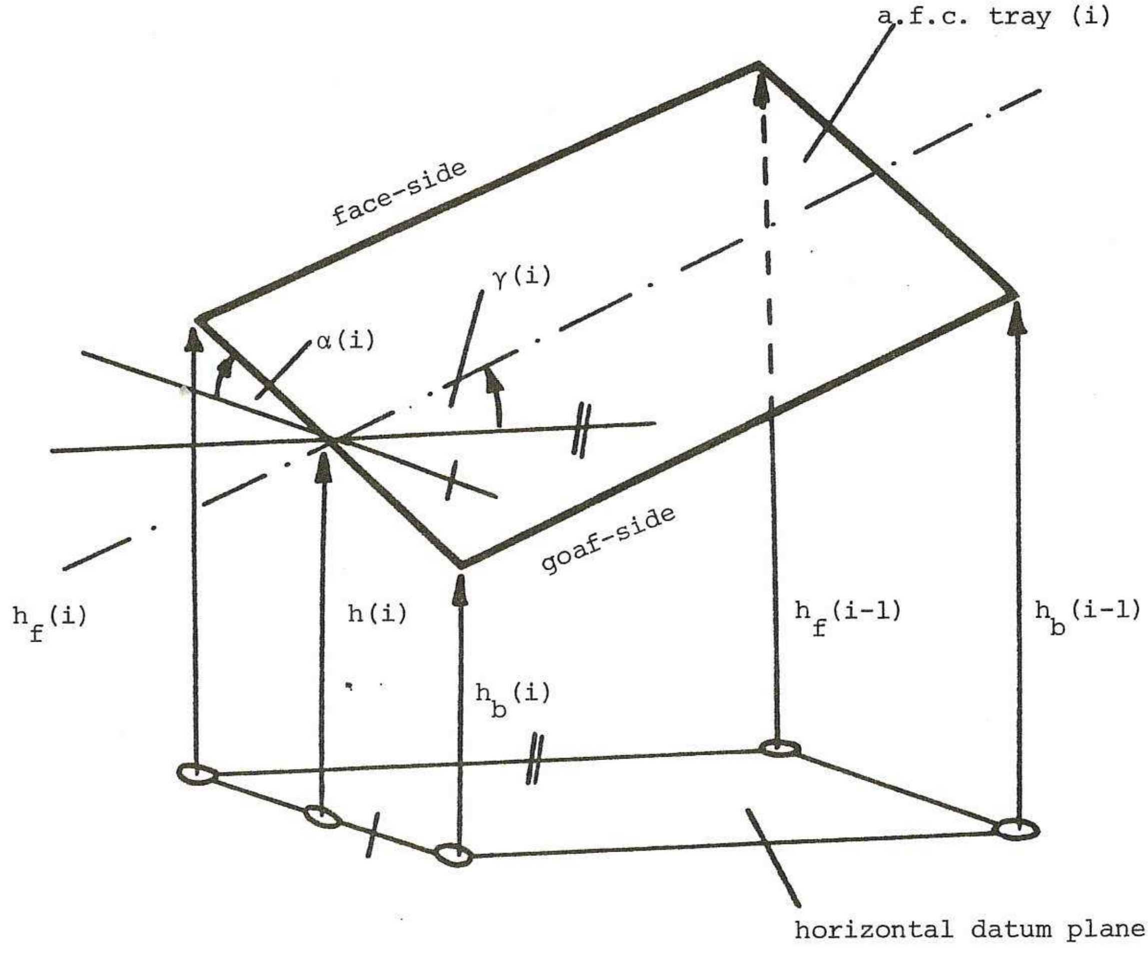

Fig. 12. Coordinates of ith tray of a.f.c

Fig. 13 Flowchart for fitting ith pan by three-dimensional dynamic programming